HEAT PRODUCTION SIMULATION AND HEAT-FORCE COUPLE ANALYSIS OF FSW PIN

C. Xue[1*] – Q. Zhang[2] – X. Ren[3]

[1] College of Science, North University of China, Taiyuan 030051; China
[2] Welding research center, North University of China, Taiyuan 030051; China

ARTICLE INFO	Abstract:
	Heat production of friction stir welding (FSW) is a fundamental phenomenon that affects the welding quality. Early studies have been focused on investigating and understanding the heat production and temperature distribution of the welding plate. However, very few studies have been done to analyze the stress of the welding pin with reference to heat-force coupling, which is of great significance for the welding pin design. Therefore, this paper sets out to analyze the heat-force coupling effect of the welding pin. Firstly, considering the variation of heat conduction coefficient at different temperatures, the temperature distribution of both aluminum alloy 2A12 and copper plate were calculated for the FSW process. The temperature distribution results are then used to analyze the heat-force coupling of FSW pin referring to the cross force and axial pressure on the welding pin. The cross force and axial pressure are determined by the softened base metal which has different mechanical properties at different temperatures. The results show that the peak value of stress is at the boundary between the shoulder and pin. The pin is liable to break at peak stress, and hence more attention should be paid to welding tool design.

1 Introduction

Friction stir welding (FSW), developed at the Welding Institute (TWI) in 1991 [1], is now becoming one of the most effective solid state joining processes. The joining technique has been widely applied to welding of non-ferrous metals such as aluminum and copper. L. Fourment et al. developed an ALE method to accurately simulate the three stages of the FSW process, taking into

consideration some complex coupling effects [2]. As shown in
Figure 1, the workpieces are tightly clamped together with a clamp apparatus and a non-consumable rotating welding tool is plunged into the abutting workpieces that are to be joined. The welding tool consists of two functional areas, the tool shoulder and the tool pin. Under the action of a vertical axial force imposed by the shoulder of the tool, the pin is forced into the workpieces and

---

[*] Corresponding author. Tel.: + 86 0351 3922150; fax: + 86 0351 3922150
E-mail address: xuechunxia@nuc.edu.cn

frictional heat is generated between the welding tool and the welded material. The frictional heat softens the material around the welding pin. Then, the welding pin is moved along the weld direction to form the weld bead with an improved metallurgical structure.
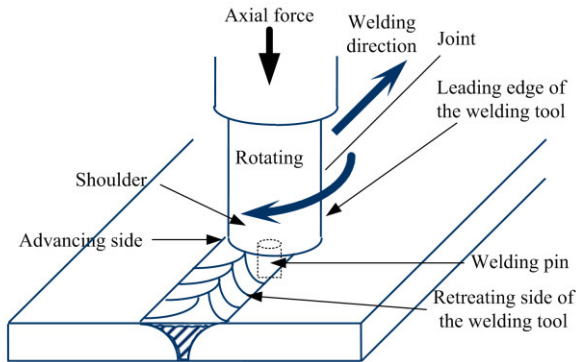

Figure 1. A schematic diagram of friction stir welding.

In friction stir welding process, the heat generated by friction and deformation flows into the workpiece as well as the tool [3]. The amount of heat conducted into the workpiece determines the quality of the weld, residual stress, distortion of the workpiece and the microstructure of the metal [4, 5]. The amount of heat that flows to the tool dictates the life time of the tool and the capability of the tool to perform the joining process. Therefore, an understanding of the heat transfer and temperature distribution in the FSW process is extremely important for improving the process. Earlier research works have proved that the shape of the welding tool determines the heat generated [6]. Therefore, the geometry of the welding tool is critical in the friction stir welding process. Even though most of the heat is generated by the shoulder, the welding pin affects the flow of the plastic material and has a significant influence on the temperature distribution of the weld seam [7, 8]. Because of the very high tangential velocities and temperatures, it is almost impossible to derive a simple experimental representative friction test for this process. Therefore, numerical simulation is a good solution for understanding the process and helping design the FSW tools [9, 10].

It is worth noting that the former research work was less focused on the heat-force coupling effect of the FSW pin, which is of great significance for welding pin design [11]. For instance, insufficient heat from friction could lead to breakage of the welding pin

since the material is not soft enough. In this paper, simulation work is done to study the heat production, stress distribution of the welding pin for friction stir welding of both aluminum alloy 2A12 and copper. A two-step approach is undertaken in the numerical analysis. First, the temperature distribution of the welding plate is computed under different given conditions, such as welding speed and rotating speed of the welding pin. Then, using the temperature distribution, the stress of the welding pin is analyzed considering force-heat coupling effect, which provides some information for welding pin design.

2 Heat production and temperature distribution analysis

Both aluminum alloy 2A12 and copper are analyzed in our research work. However, the simulation processes for alloy 2A12 and copper are basically the same. Therefore, the simulation process of only aluminum alloy 2A12 is described whereas the simulation results of both alloy 2A12 and copper are introduced for comparison.

2.1 Simulation process for heat production

An aluminum alloy 2A12 plate with size 120 mm ×50 mm ×4 mm is used as the welded metal. As shown in Fig. 2, the FSW tool made of tool steel H31 has a flat shoulder radius (R_s) of 15mm, a cylindrical pin radius (R_p) of 3.6 mm and a pin length (H_p) of 3.8 mm.
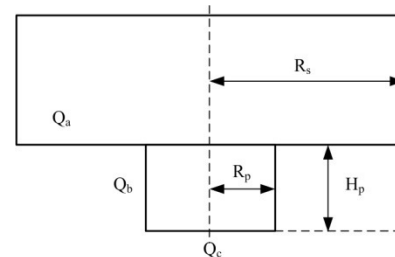

Figure 2. Shape of a welding pin.

The axial force of the welding pin is 2 kN. Four different process conditions are used for the welding process simulation:
a) Rotational speed of the welding pin $\omega = 850$ rmp, welding speed $v = 36$mm/min;
b) Rotational speed of the welding pin $\omega = 850$ rmp, welding speed $v = 60$ mm/min;

c) Rotational speed of the welding pin ω = 1200 rmp, welding speed v = 36 mm/min;
d) Rotational speed of the welding pin ω = 1200 rmp, welding speed v = 60 mm/min;

2.1.1 Heat source model

The total heat production during the FSW process is generated by the friction energy and plastic deformation of the welded metal. For the energy produced by plastic deformation and the flow of the welded metal, it is only important to use the threaded welding pin. For the flat welding pin, which is used in our simulation work, the energy generated by plastic deformation can be neglected. Therefore, the total heat (Q) is composed of the frictional heat generated by the shoulder (Q_a) and the welding pin (Q_b+Q_c). The heat generated by the tip surface of the welding pin (Q_c) is very small in comparison with Q_a and Q_b, which exerts less effect on the temperature distribution. Therefore, only Q_a and Q_b are considered in our simulation work.
Heat generated at infinitesimal area dA, with a distance of r from the rotating axis is given as:

$$dQ = \omega dM = \omega r \tau dA \qquad (1)$$

where M stands for the torque caused by the friction force according to the rotating axis; ω is the rotational speed; τ is the friction stress.
Then, we can get the energy produced by the shoulder in one unit movement.

$$Q_a = \int_{2\pi r}^{0} d\tau dl = \frac{4\pi\omega\mu F\left(R_s^3 - R_p^3\right)}{3v\left(R_s^2 - R_p^2\right)} \qquad (2)$$

where F is the axial force of the FSW tools (N), which is determined by the welding condition. μ is the friction coefficient, which is determined by the material properties. For Q_b, the back side of the welding pin contacts with the high temperature soften base metal, which has a very small friction coefficient. Therefore, only the front side of the welding pin is taken into account for the heat generation. The energy generated by the welding pin is given as:

$$Q_b = \int_{\pi r}^{0} d\tau dl = \frac{\pi^2\mu\sigma_z\omega LR_p^2}{v} \qquad (3)$$

σ_z is the side stress of the welding pin, which is equal to the yield stress of the soften welded material (Pa).

2.1.2 Governing equation and the boundary condition

The friction stir welding process is a typical non-linear instant heat conduction process. The Fourier equation and the law of conservation of energy are used to get the governing equation (see Equation 4) for the three dimensional temperature field.

$$\rho c \frac{\partial T}{\partial t} = \frac{\partial}{\partial x}\left(k_x \frac{\partial T}{\partial x}\right) + \frac{\partial}{\partial y}\left(k_y \frac{\partial T}{\partial y}\right) + \frac{\partial}{\partial z}\left(k_z \frac{\partial T}{\partial z}\right) + Q \qquad (4)$$

where, T is temperature (K), t is time (s), ρ is density of the material (Kg/m^3), C is the specific heat capacity (J/Kg·°C), Q is inner heat source (W/m^3), k_x, k_y, k_z is the material conductivity in x, y, z direction (W/m^2·°C). The initial temperature is given as:

$$T\left(x, y, x, t\right)\big|_{t=0} = T\left(x, y, z\right) = T_\infty \qquad (5)$$

where, T_∞ is the environment temperature. The boundary between welding tool and the work plate is set as:

$$k\frac{\partial T}{\partial n}\big|_\Gamma = q_i \qquad (6)$$

q_i stands for the heat flux between the friction tool and the weldment, whereas n is the normal vector of boundary Γ. The boundary between the work plate and the air is set as:

$$k\frac{\partial T}{\partial n}\big|_\Gamma = \gamma(T - T_\infty) \qquad (7)$$

γ stands for the convection coefficient. The thermophysical properties of welded metal aluminum alloy 2A12 are given in Table 1.

_____

Table 1. Thermophysical properties of aluminum alloy 2A12 at different temperatures

Temperature (T/°C)	20	100	200	300	400
Specific heat capacity (C/J·Kg^{-1}·°C^{-1})	921	921	1047	1130	1172
Thermal conductivity (λ/ W·m^{-1}·°C^{-1})	128	134	151	172	176

2.2 Temperature field simulation results

After about 20 s of the welding process, the temperature field will be stable and the simulation results of aluminum alloy 2A12 are shown in Fig.3 to Fig. 6. As shown in Fig. 3, for ω = 850 rmp and υ = 36 mm/min, the highest temperature is at the contact surface of the shoulder and welding pin with the value about 404 °C. The results agree well with the experimental result [12~14]. The similar temperature field can be observed for the other three welding conditions (Fig. 4 ~ Fig. 6).

However, by increasing welding speed, the linear energy input is decreased, which leads to a lower temperature distribution. As shown in Fig. 4, the highest temperature is only about 346 °C comparing with the 404 °C in Fig. 3. The same phenomena can also be observed in Fig. 5 and Fig. 6. When the rotating speed is increased, the heat input is also increased, which leads to higher temperature. As shown in Fig. 3 and Fig. 5, when the rotating speed is increased from 850rmp to 1200rpm, the maximum temperature is increased from 404 °C to 523 °C. The difference of maximum temperature and temperature distribution will exert a significant effect on the heat-force coupling analysis of the welding pin. Therefore, the welding parameter is a deciding factor for the state of the welding process, which is significant for the quality of the weld bead and life time of the friction stir welding tools.

Apart from analyzing the FSW process of aluminum alloy 2A12, we also analyze the FSW process of copper with the same method. The simulation results are thus given so as to compare the welding process of different welded metals, and to provide some information on the welding tool design based on the welded metal. As shown in Fig. 7, the maximum temperature of 828 °C can be reached in copper welding, which is higher than aluminum welding.
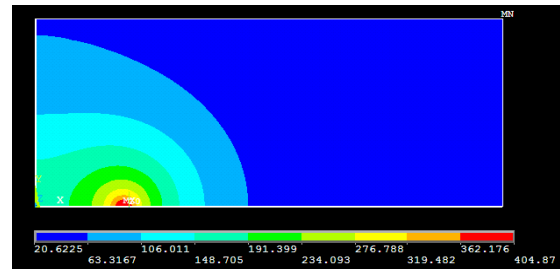

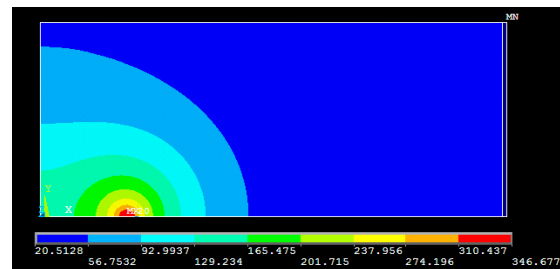*Figure 3. 850 rpm Rotational speed, 36 mm/min welding speed.*

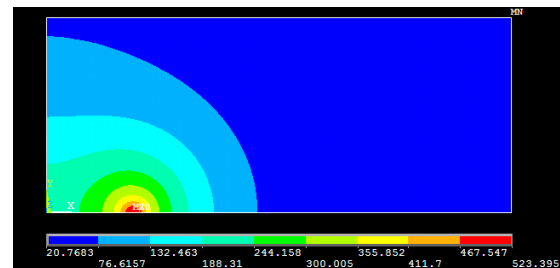*Figure 4. 850 rpm rotational speed, 60 mm/min welding speed.*

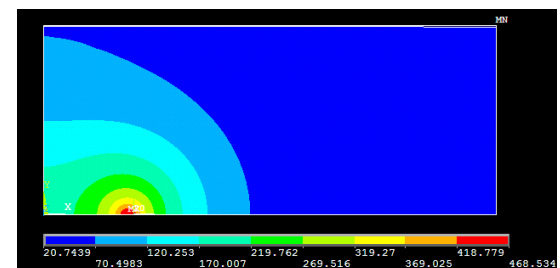*Figure 5. 1200 rpm rotational speed, 36 mm/min welding speed.*

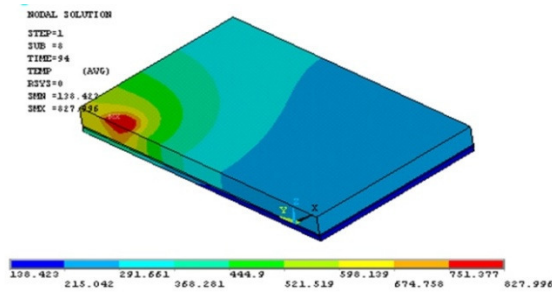*Figure 6. 1200 rpm Rotational speed, 60 mm/min welding speed.*

Figure 7. Temperature distribution of welded copper plate.

3 Heat-force coupled analysis of welding pin

3.1 Simulation model for heat-force couple analysis

As previously discussed, the welding pin that can be broken under improper welding parameters is important for the FSW process. Therefore, it is necessary to analyze the stress of the welding pin with respect to heat-force coupling. As the welding pin works at high temperature due to the heat transferred from the softened weld beam to the welding pin, the material required for the heat-force coupling simulation must be at high temperature. The material mechanical properties of both the welding tool (chisel tool steel H13) and the welded metal (aluminum alloy 2A12) at different temperatures are shown in Table 2 and Table 3.

Table 2. Properties of the welding tool (chisel tool steel H13)

Temperature (T/°C)	20	200	400	600
Modulus of elasticity (10^{11}Pa)	2.06	1.92	1.75	1.53
Poisson ratio	0.3	0.3	0.3	0.3

Table 3. Yield strength of aluminum alloy 2A12

Temperature (T/°C)	20	200	300
Yield strength (Pa)	410	325	265

In order to get a better accuracy and optimize the calculation results, the non-uniform mesh is used to simulate the heat-force couple of the friction stir welding tool. As shown in Fig. 8a, the mesh at the root of the welding pin is thick and the other part is

thin. The welding pin is assumed to be statistic in the coordinate system. According to the welding condition, the axial force of the welding pin is supposed to be 2 kN and the cross force is related to the temperature and properties of the softened weld metal.
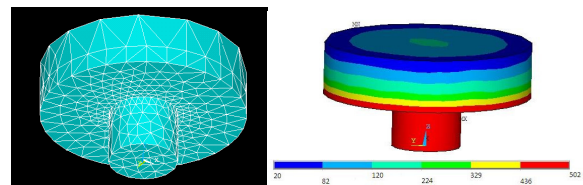

Figure 8. Mesh and temperature distribution of the welding pin.

Taking into consideration the heat loss due to heat transfer conduction, convention and radiation, the simulated temperature distribution of the welding pin is shown in Fig. 8b. For the shoulder and the welding pin, the contact surface with the welded material is set to be in agreement with the temperature field as well as that of the weld bead. The environment temperature is set to be within 20 °C.

3.2 Heat stress analysis result with heat-force coupling

Heat stress is an interaction and coupling effect between the heat and stress field. ANSYS provides two methods for heat stress analysis, the direct and indirect method. The indirect method is applied in the simulation work of this paper. Based on the thermal analysis, the indirect method puts the acquired temperature on the stress structure as a cubic load.

Figure 9 provides the stress distribution of the welding pin at 4 s for the welding process with 120 rpm rotational speed and 60 mm/min welding speed. In Fig. 9, the maximum stress is about 0.6×10^{10} Pa on the connecting part between the shoulder and welding pin, which is subjected to the cross extrusion force and the pressure of Z direction. More attention should be paid to the strength of this part when designing the welding pin. Comparing with the stress distribution at 4 s (Fig. 9), the maximum stress distribution at 20 s (Fig. 10) is about 0.475×10^{10} Pa, which is obviously smaller than that at 4 s. This helps to explain the phenomena/phenomenon that the welding pin is

liable to break at the early stage of the welding when the heat input is not enough to soften the weld metal. For a lower welding speed at 36 mm/min (Fig. 11), the maximum stress is about 0.46×10^{10} Pa, which is smaller than that in Fig. 9. Welding speed is a key factor for determining the maximum welding pin stress, if temperature is not high enough to soften the weld metal. Higher welding speed and lower rotating speed mean lower linear energy input, which can cause welding (seam) defects and the welding tool to be out of work/service. Therefore, by analyzing the heat production and stress distribution of the welding pin, an optimized parameter can be suggested for friction stir welding with specific welded metal.

In order to further study the influence of welded metal on the welding pin stress, the stress distribution of the welding pin for copper welding is also provided in Fig. 12. For copper welding, the maximum stress at 20 s is about 0.64×10^{10} Pa, which is higher than that of aluminum welding. This is important for welding pin design and material selection since they both depend on the properties of welded metal.

Therefore, both welding parameters and properties of the welded metal have great influence on the application of FSW tools. The simulation result can help select the material used for FSW tool and the proper welding parameter for its application.
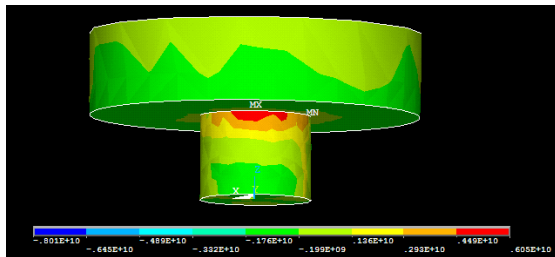

Figure 9. The stress distribution of welding pin at 4 s with 1200 rpm and 60 mm/min.
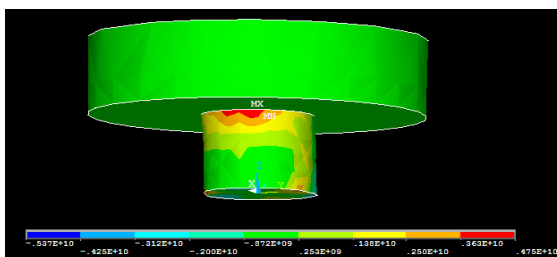

Figure 10. Stress distribution of welding pin at 20 s with 1200 rpm and 60 mm/min.
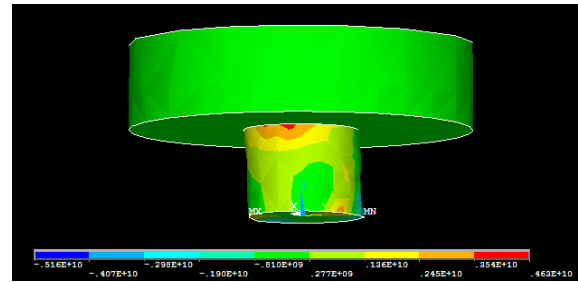

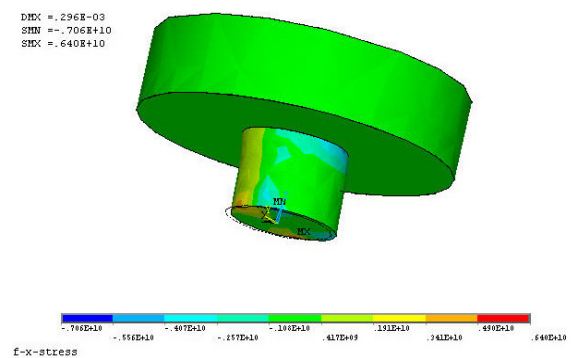*Figure 11. The stress distribution of welding pin at 20s with 1200rpm and 36mm/min.*

Figure 12. The stress distribution of welding pin for copper welding.

4   Conclusion

1. The friction stir welding parameters exert a significant influence on the temperature field of the welding plate. By increasing rotating speed and decreasing welding speed, the linear heat input is increased, which result in higher temperature distribution.

2. The differences of maximum temperature and temperature distribution have a significant effect on the heat-force coupling analysis of the welding pin. Welding speed is a key factor for determining the maximum welding pin stress. The properties of welded metal are also very important for a/the design of the welding tool.

Acknowledgements

_____

References

[1] Zhang, H., Lin, S.B., Wu, L.: *Mechanical properties of friction stir welds on AZ31 magnesium alloy,* Transition of the China Welding Institute, 24 (2003), 5, 91-96.

[2] Fourment, L., Guerdoux, S.: *3D numerical simulation of the three stages of Friction Stir Welding based on friction parameters calibration*, International Journal of Material Forming, 1 (2008), s1, 1287-1290.

[3] Ji, S.D., Shi, Q.Y., Zhang, L.G. et al.: *Numerical simulation of material flow behavior of friction stir welding influenced by rotational tool geometry*, Computational Materials Science, 63 (2012), 10, 218-226.

[4] Prasanna, P., Rao, B. S., Rao, G.K.M.: *Finite element modeling for maximum temperature in friction stir welding and its validation*, International Journal of Advanced Manufacturing Technology, 51 (2010), 9-12, 925-933.

[5] Simar, A., Brechet, Y., de Meester, B. et al.: *Integrated modeling of friction stir welding of 6xxx series Al alloys: Process, microstructure and properties,* Progress in Materials Science, 57 (2012), 1, 95-183.

[6] Hirasawa, S., Badarinarayan, H., Okamoto, K. et al.: *Analysis of effect of tool geometry on plastic flow during friction stir spot welding using particle method,* Journal of Material Processing Technology, 201 (2010), 11, 1455-1463.

[7] Zhao, Y. H., Lin, S. B., Wu, L.: *The influence of pin geometry on bonding and mechanical properties in friction stir weld 2014 Al alloy,* Materials Letters, 59 (2005), 23, 2948-2952.

[8] Boz, M., Kurt, A.: *The influence of stirrer geometry on bonding and mechanical properties in friction stir welding process,* Material and Design, 25 (2004), 4, 343-347.

[9] Liu, H.J., Feng, J.C., Fujii, H.: *Wear characteristics of a WC-Co tool in friction stir welding of AC4A+30 vol%SiCp composite,* International Journal of Machine Tools and Manufacture, 45 (2005), 14, 1635-1639.

[10] Lin, S.B., Zhao, Y.H., He, Z.Q. et al.: *Modeling of friction stir welding process for tools design,* Frontiers of Material Science, 5 (2011), 2, 236-245.

[11] Wang, Z. Y., Zhang, Z.: *Adaptive re-meshing based numerical simulation of friction stir welding and tool force analysis,* Journal of Physics Engineering, 19 (2012), 2, 107-113.

[12] Zhang, Z., Zhang, H.W.: *Effect of contact model on numerical simulation of friction stir welding.* Acta Metallurgica Sinica, 44 (2008), 1, 85-90.

[13] Yan, D.Y., Shi, Q.Y., Wu, A.P. et al.: *Numerical analysis on the residual distortion of Al alloy sheet after friction stir welding,* Acta Metallurgica Sinica, 45 (2009), 2, 183-188.

[14] Zhang, Z., Bie, J., Liu, Y. L. et al.: *Effect of traverse/rotational speed on material deformations and temperature distributions in friction stir welding,* Journal of Mater Science and Technology, 24 (2008), 6, 907-914.